Vol. 09, No. 02 (2025) 137 – 149
JIIF (Jurnal Ilmu dan Inovasi Fisika)
https://jurnal.unpad.ac.id/jiif/

EFFECT OF CALCINATION TEMPERATURE ON THE CRYSTALLITE SIZES AND STABILITY OF ZNO NANOPARTICLES SYNTHESIZED VIA GREEN METHOD USING MELALEUCA LEUCADENDRA(L) LEAF EXTRACT

INTAN SOPHIA CAHYANI[1], DEVI NURMALASARI[1], CAMELLIA PANATARANI[1,2,*]

[1]*Departement of Physics, Faculty of Mathematics and Natural Sciences, Universitas Padjadjaran Jl. Raya Bandung-Sumedang Km.21 Jatinangor 45363, West Java, Indonesia, Telp. 022-7796014*
[2]*Functional Nano Powder University Center of Excellence, Universitas Padjadjaran, Jalan Raya Bandung-Sumedang KM 21, Jatinangor 45363, West Java, Indonesia*

**Corresponding author*
Email: c.panatarani@unpad.ac.id

Submitted: 02/04/2025
Accepted: 05/04/2025
Published: 06/08/2025

Abstract. Synthesis of zinc oxide (ZnO) nanoparticles is a growing research field with wide applications in electronic equipment, pharmaceuticals, optics, and food packaging. This study aims to investigate the effect of calcination temperature on the cristallite size and stablity of ZnO nanoparticles synthesized by the sol-gel method with and without the addition of *Melaleuca leucadendra*(L) leaf extract. The calcination process was carried out at temperatures of 400°C, 600°C, and 800°C. Sample characteristics were observed using XRF, FTIR, XRD, PSA, ZETA, and PL. XRD characterization showed that all samples had a hexagonal wurtzite crystal structure, with increasing temperature resulting in higher crystallinity and larger crystallite sizes, reaching 78.71 nm at 800°C for the sample without extract and 32.81 nm for the sample with extract. PSA analysis showed that the particles with extract had a more uniform size distribution, especially at 800°C. The zeta potential values ranged from -43mV to -57mV, indicating good colloidal stability. UV-Vis spectra showed that the energy of the exclusion band (Eg) increased with temperature, with the highest value (3.52eV) in the sample without extract at 800°C. These results indicate that the calcination temperature plays a crucial role in improving the crystal quality and particle stability. Meanwhile, the addition of eucalyptus leaf extract acts as a natural stabilizing agent that helps reduce crystal defects.

Keywords: ZnO nanoparticles, calcination temperature, eucalyptus leaf extract, crystal size, particle stability

Abstrak. *Sintesis nanopartikel seng oksida (ZnO) merupakan bidang penelitian yang berkembang pesat dengan berbagai aplikasi luas dalam peralatan elektronik, farmasi, optik, dan pengemasan makanan. Penelitian ini bertujuan untuk menyelidiki pengaruh temperatur kalsinasi terhadap ukuran kristalit dan stabilitas nanopartikel ZnO yang disintesis menggunakan metode sol-gel, baik dengan maupun tanpa penambahan ekstrak daun kayu putih Melaleuca leucadendra(L). Proses kalsinasi dilakukan pada temperatur 400°C, 600°C, dan 800°C. Karakterisasi sampel dilakukan menggunakan XRF, FTIR, XRD, PSA, zeta potential, dan fotoluminesensi (PL). Hasil karakterisasi XRD menunjukkan bahwa semua sampel memiliki struktur kristal wurtzit heksagonal, di mana peningkatan temperatur menghasilkan kristalinitas yang lebih tinggi dan ukuran kristalit yang lebih besar, yaitu*

DOI: https://doi.org/10.24198/jiif.v9i2.64982 *e-ISSN: 2549-7014*

mencapai 78,71 nm pada suhu 800°C untuk sampel tanpa ekstrak dan 32,81 nm untuk sampel dengan ekstrak. Analisis PSA menunjukkan bahwa partikel dengan ekstrak memiliki distribusi ukuran yang lebih seragam, terutama pada suhu 800°C. Nilai zeta potential berkisar antara -43 mV hingga -57 mV, yang menunjukkan stabilitas koloid yang baik. Spektrum UV-Vis menunjukkan bahwa energi pita larangan (Eg) meningkat seiring dengan kenaikan temperatur, dengan nilai tertinggi (3,52 eV) pada sampel tanpa ekstrak pada suhu 800°C. Hasil ini menunjukkan bahwa temperatur kalsinasi berperan penting dalam meningkatkan kualitas kristal dan stabilitas partikel. Sementara itu, penambahan ekstrak daun kayu putih berfungsi sebagai agen penstabil alami yang membantu mengurangi cacat kristal.

Kata kunci: *Nanopartikel ZnO, suhu kalsinasi, ekstrak daun kayu putih, ukuran kristal, stabilitas partikel*

1. Introduction

Zinc oxide (ZnO) is a type II and VI semiconductor material that has a wide band gap of 3.37 eV and a bond energy of 60 MeV [1]. ZnO is a powdery inorganic material that is difficult to dissolve in water. The advantages of ZnO material include its wide band gap. The band gap is the energy required to move an electron from the valence band to the conduction band; a wide band gap allows it to exhibit strong exciton binding energy, high thermal stability, and efficient UV absorption [2]. Additionally, ZnO exhibits significantly higher electron mobility (~100-300 $cm^2/V \cdot s$) compared to many other metal oxides, such as TiO_2 (0.1-4.0 $cm^2/V \cdot s$), improving charge transport efficiency in devices like sensors and photocatalysts [3]. Beyond semiconductor technologies, ZnO powder serves as a versatile additive in the manufacturing of ceramics, rubbers, plastics, cement, glass, and lubricants, due to its biocompatibility, low cost, and multifunctional properties [1].

The success in making ZnO nanoparticles must consider several factors, including the source of the base. capping agent and the synthesis method used. The methods commonly used in the synthesis of metal oxide nanoparticles are the mechanical method, by produces nano-sized particles [4], spray pyrolysis [5], sonochemical [6], hydrothermal [7], and sol-gel method [8]. Among these methods, the sol-gel method was chosen in this study because it offers good solution homogeneity, particle size control, high purity, and low temperature reaction conditions [9].

In conventional synthesis, reducing and stabilizing agents such as hexamine and NaOH [10] are commonly used, but they are toxic and not environmentally friendly. Therefore, green synthesis approaches have been developed. This approach uses natural materials as base sources and capping agents, such as Nilgiri Antusciliantus leaf extract, Syzygium cumini, Azadirachta indica, Punica granatum fruit peel, and Ficus religiosa leaves [11]. In addition to reducing the use of hazardous chemicals, green synthesis also offers a simple, cost-effective, and environmentally friendly process. In this context, eucalyptus *Melaleuca leucadendra*(L) leaf extract has great potential as a natural reducing and stabilizing agent in ZnO synthesis. This plant is known as a source of essential oil (cajuput oil) and grows widely in eastern Indonesia and Australia. The leaves contain active compounds such as 1,8-cineol, α-terpineol, α-pinene, limonene, globulol, and guaiol which have been shown to have high antioxidant activity [12]. These compounds can act as reducing agents as well as stabilizers during the nanoparticle formation process.

Various previous studies have reported the successful synthesis of ZnO nanoparticles using plant extracts through green methods, such as Eucalyptus lanceolata (leaf litter) [13], Eucalyptus globulus in the CuO/ZnO system [14], as well as various other Eucalyptus species [15]. Although various studies have reported the successful synthesis of ZnO nanoparticles using plant extracts through green methods, some previous studies focused more on variations in extract concentration or reaction pH, without further exploring how calcination temperature affects ZnO characteristics. Increasing the calcination temperature can improve the regularity of the crystal structure, increase the crystallite size, and reduce crystal defects, resulting in more stable and stronger optical and photoluminescence properties. However, this effect has not been widely studied in *Melaleuca leucadendra*(L) leaf extract-based systems, which contain unique active biomolecules such as 1,8-cineole and globulol.

Therefore, this study aims to investigate the effect of calcination temperature variation on the crystal structure, particle size, colloidal stability, and optical properties of ZnO nanoparticles synthesized via the sol-gel method using *Melaleuca leucadendra*(L) leaf extract. Hopefully, this approach can produce high-quality ZnO nanoparticles through an environmentally friendly and sustainable process.

2. Research Methods

2.1 Materials

Zinc nitrate hexahydrate ($Zn(NO_3)_2 \cdot 6H_2O$, ≥98%) was purchased from Merck and used as the zinc precursor. Distilled water (aquadest) was used as the solvent throughout the synthesis. Fresh leaves of *Melaleuca leucadendra*(L) were collected from local sources in Indonesia and used for the preparation of leaf extract.

2.2 Preparation of Herbal Cajuput Leaf Extract

This process was carried out to extract the chemical constituents from the plant material and obtain the bioactive compounds contained within. In this study, the cajuput *Melaleuca leucadendra*(L) leaf extract were first ground into smaller pieces. The extraction was performed using a decoction method, in which 20 grams of ground cajuput leaves were heated with 100 mL of distilled water at 60°C for 20 minutes. After heating, the resulting extract was filtered using Whatman No. 1 filter paper to separate the plant residue from the liquid extract. The obtained extract was then stored in a sealed container and refrigerated for further use. Refrigeration was necessary to prevent oxidation and preserve the extract's bioactive compounds.

2.3 Green Synthesis Procedure

Two green synthesis routes were carried out with and without using plant extract. For the synthesis involving the plant extract, 20 mL of *Melaleuca leucadendra*(L) (cajuput) leaf extract was first taken and heated while stirring on a magnetic heating stirrer at a temperature of 60°C to 80°C. Once the extract reached 60°C, 2 grams of the precursor zinc nitrate hexahydrate ($Zn(NO_3)_2 \cdot 6H_2O$) were added. The mixture was continuously heated until the solvent evaporated, resulting in a viscous paste. This paste was then transferred into a ceramic crucible for subsequent calcination in a furnace. The synthesis was performed three times at different calcination temperatures of 400°C, 600°C, and 800°C, each for 2 hours. For the synthesis without the plant extract, 10 grams of zinc nitrate hexahydrate ($Zn(NO_3)_2 \cdot 6H_2O$) were directly placed into a ceramic crucible and

calcined under the same temperature and duration conditions as those used in the synthesis with the extract.

2.4 Characterization of ZnO Nanoparticles

The synthesized ZnO powder was then characterized using several analytical techniques. X-ray Fluorescence (XRF) spectrometry was used to analyze the chemical composition and elemental concentrations within the samples. X-ray Diffraction (XRD) was employed to identify the crystal structure of the samples. Fourier Transform Infrared (FTIR) spectroscopy was carried out to identify functional groups present in both the plant extract and the synthesized ZnO nanoparticles. Particle Size Analysis (PSA) and Zeta Potential (ZP) measurements were performed using the Dynamic Light Scattering (DLS) technique to determine particle size distribution and surface charge, respectively. Photoluminescence (PL) spectroscopy was conducted at an excitation wavelength of 254 nm to determine the emission wavelength of the samples

3. Results and Discussion

3.1 XRF Analysis

The elemental composition data obtained from X-ray fluorescence (XRF) analysis for ZnO samples synthesized with and without the addition of plant extract at three different calcination temperatures are presented in Table 1.

Table 1. Chemical Element Composition of Sample from XRF Characterization

Material	Element	Temperature calcination 400^{o}C		Temperature calcination 600^{o}C		Temperature calcination 800^{o}C	
		Mass (%)	Atomic (%)	Mass (%)	Atomic (%)	Mass (%)	Atomic (%)
ZnO without extract	Zn	60.3	31.64	88	42.06	81.2	52.3
	O	39.1	68.09	11.4	27.7	18.1	47.3
ZnO with extract	Zn	92.2	86.8	92.6	88.5	95.2	94
	O	3.26	5.11	3.08	4.34	1.87	2.32

The elemental composition data obtained from X-ray fluorescence (XRF) analysis for ZnO samples synthesized with and without the addition of plant extract at three different calcination temperatures are presented in Table 1. The main elements detected were zinc (Zn) and oxygen (O), consistent with the typical composition of ZnO. For the ZnO samples synthesized without extract, at all calcination temperatures (400°C, 600°C, and 800°C), the atomic composition showed that the Zn content was lower than that of O. At 400°C, the atomic Zn:O ratio was close to the ideal stoichiometric value of 1:1, with a measured ratio of approximately 0.46. However, at 600°C and 800°C, the ratios increased to 1.52 and 1.11, respectively. This increase may be attributed to oxygen loss during the calcination process [16]. The higher Zn:O ratio suggests the possible formation of structural defects such as oxygen vacancies (V_O) or zinc interstitials (Zn_i), which can influence the electronic and optical properties of the material.

In contrast, ZnO samples synthesized with the addition of plant extract exhibited significantly higher Zn:O atomic ratios, reaching 18.9 at 400°C and increasing to 40.4 at 600°C, before decreasing to 6.5 at 800°C. These highly imbalanced ratios indicate that

the presence of extract during synthesis may lead to substantial oxygen depletion in the ZnO structure. This phenomenon is likely due to the reductive activity of organic compounds present in the extract during thermal treatment, which may enhance the formation of defects such as Zn interstitials or oxygen deficiencies. Previous studies have reported that reductive conditions during calcination can increase the concentration of such defects [16].

3.2 FTIR Analysis of Plant Extract and ZnO Nanoparticles

Figure 1 presents the FTIR spectrum of the cajuput *Melaleuca leucadendra*(L) leaf extract. The spectra of both the extract and the synthesized ZnO nanoparticles were examined to identify the functional groups derived from biomolecules in the extract, which may act as reducing and stabilizing agents during nanoparticle formation.

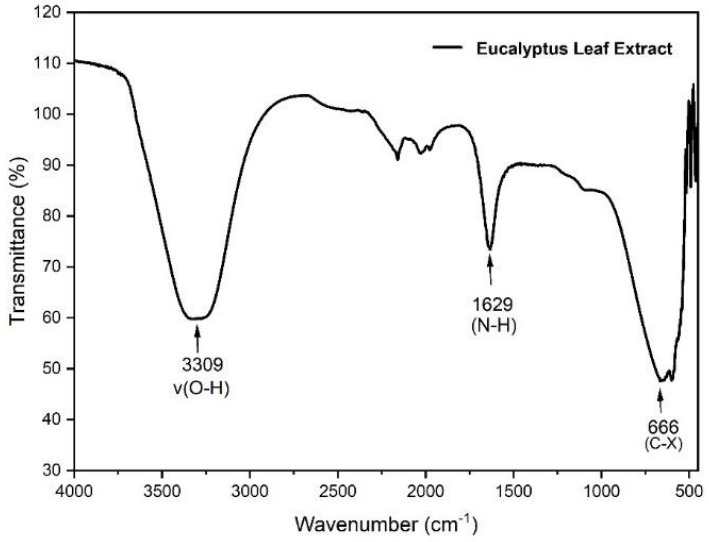

Figure 1. FTIR spectrum of *Melaleuca leucadendra*(L) leaf extract

The broad and intense absorption band observed around 3309 cm^{-1} can be attributed to the stretching vibration of hydroxyl (–OH) groups, commonly found in phenolic and alcoholic compounds [17]. The presence of these groups suggests that polyphenols, flavonoids, or tannins are present in the extract. The absorption band at 1629 cm^{-1} is associated with the stretching vibrations of amine groups (N–H from NH_2) or C=C double bonds, which may originate from unsaturated organic compounds such as proteins, alkaloids, or other phenolic constituents [17]. Meanwhile, the small peak observed at 666 cm^{-1} corresponds to the stretching vibration of C–X bonds, where X represents a halogen element [18]. Although its presence reflects the chemical complexity of secondary metabolites present in the natural extract.

3.3 FTIR Spectra of ZnO Samples Synthesized with and without Plant Extract

Figure 2 presents the FTIR spectra of ZnO samples synthesized without (S1–S3) and with (S4–S6) the addition of *Melaleuca leucadendra*(L) leaf extract at calcination temperatures of 400°C, 600°C, and 800°C. In Figure 2a, the samples without extract (S1-S3) do not exhibit the characteristic Zn-O stretching band, which typically appears in the wavenumber region of 400-600 cm^{-1}. The absence of this feature suggests that the formation of the ZnO crystal structure was not fully achieved. This may be due to the lack of reducing and stabilizing agents provided by biomolecules, which play a crucial

role in facilitating the transformation of Zn precursors into ZnO under thermal conditions. The resulting spectra predominantly reflect residual inorganic compounds from the precursor rather than the presence of specific functional groups indicative of ZnO nanoparticle formation [19].

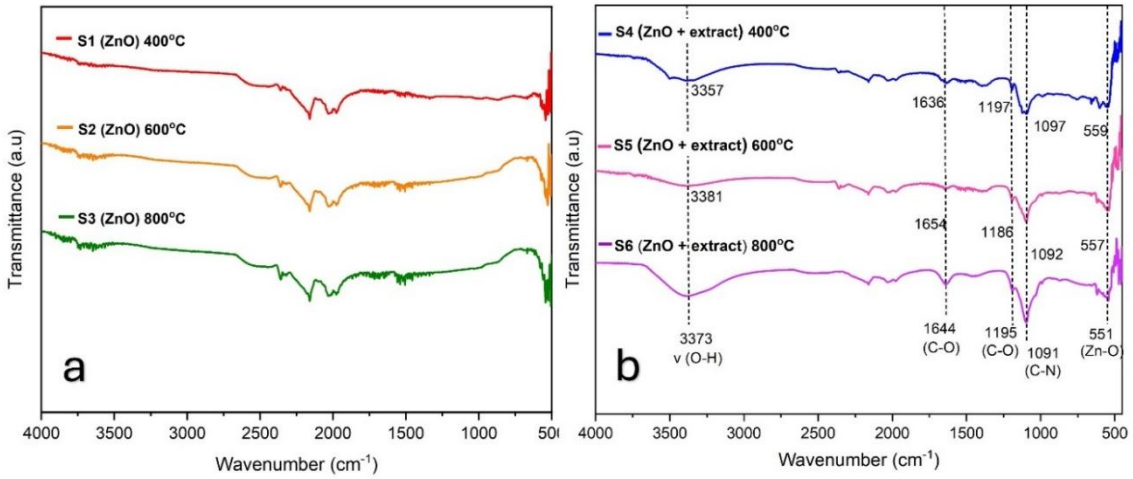

Figure 2. FTIR spectra of ZnO samples without extract (Figure 2a) and with *Melaleuca leucadendra*(L) leaf extract (Figure 2b) at 400°C, 600°C, and 800°C calcination temperature variations.

In contrast, as shown in Figure 2b, the samples synthesized with the plant extract (S4–S6) display significant spectral changes. Absorption bands in the range of 3357–3381 cm^{-1} correspond to O–H stretching vibrations, indicating the presence of phenolic and alcoholic compounds from the plant extract. The intensity of these bands decreases with increasing calcination temperature, reflecting the decomposition of organic compounds. The absorption bands at 1636–1654 cm^{-1} are attributed to the stretching vibrations of carbonyl (C=O) groups or N–H bending vibrations from amines, likely originating from proteins or flavonoids in the extract [20]. These functional groups are essential in the biosynthesis of ZnO nanoparticles, acting as both reducing and stabilizing agents. Additional bands observed at 1186–1197 cm^{-1} and 1091–1097 cm^{-1} are associated with the C–O stretching of primary alcohols and the C–N stretching of primary amines, respectively, indicating the involvement of organic biomolecules during nanoparticle formation [21]. Finally, the sharp absorption bands at 551–559 cm^{-1} correspond to Zn–O stretching vibrations [21], providing strong evidence of ZnO crystal structure formation, particularly in the samples calcined at higher temperatures.

3.3 XRD Analysis

Figure 3 shows the XRD diffraction patterns of all ZnO samples compared with the standard crystal database (COD No. 96-900-4180). All samples exhibit diffraction peaks consistent with the hexagonal wurtzite structure of ZnO, as confirmed by the lattice parameters ($a = b \neq c$) listed in Table 2. This indicates that the primary crystal structure of ZnO remains stable at all calcination temperatures up to 800° C, regardless of whether the synthesis was performed with or without the addition of *Melaleuca leucadendra*(L) leaf extract. Furthermore, the unit cell volume remained within a narrow range (47.54–47.72 $Å^3$), suggesting no phase transition occurred.

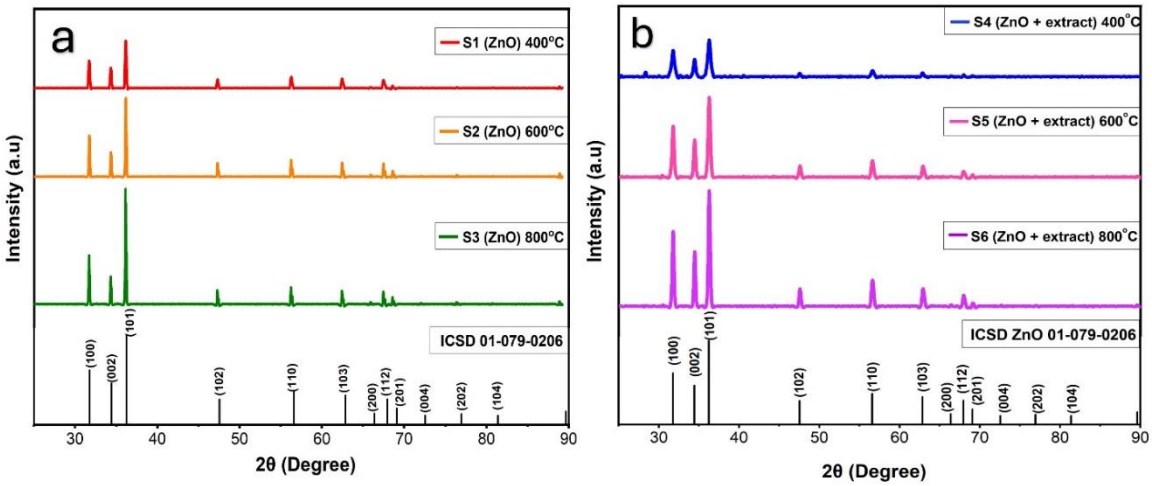

Figure 3. XRD Diffraction patterns of ZnO samples without extract (Figure 3a) and with *Melaleuca leucadendra*(L) leaf extract (Figure 3b) at 400°C, 600°C, and 800°C calcination temperature variations

As shown in Figure 3a and Table 2, increasing the calcination temperature led to sharper and narrower diffraction peaks and a reduction in Full Width at Half Maximum (FWHM) values, indicating enhanced crystallinity and crystal growth. As reported in Table 2, for the samples without extract (pure ZnO), the FWHM decreased from 0.21 to 0.12 as the temperature increased from 400°C to 800°C, while the crystallite size increased from 45.22 nm to 78.71 nm. This improvement in crystallinity is attributed to the higher thermal energy provided during calcination, which facilitates atomic rearrangement, enhances crystal order, and reduces lattice defects [22].

Table 2. Comparison of lattice parameters, crystallite size, DoC, and Cell Volume of samples

Sample	a=b (Å)	C (Å)	FWHM	Crystallite Size (D) nm	Volume Cell (Å^3)	DoC (%)
S1 (ZnO) 400°C	3.249	5.208	0.21	45.22	47.65	49.90
S2 (ZnO) 600°C	3.249	5.206	0.14	68.41	47.61	55.08
S3 (ZnO) 800°C	3.248	5.198	0.12	78.71	47.54	68.16
S4 (ZnO + extract) 400°C	3.251	5.209	0.31	28.74	47.72	57.83
S5 (ZnO + extract) 600°C	3.248	5.200	0.27	29.67	47.63	64.43
S6 (ZnO + extract) 800°C	3.247	5.200	0.24	32.81	47.61	80.60

In contrast, as illustrated in Figure 3b and Table 2, the ZnO samples synthesized with the plant extract exhibited significantly smaller crystallite sizes at the same temperatures. For instance, at 800°C, the crystallite size of pure ZnO reached 78.71 nm, whereas the sample with extract only reached 32.81 nm. This suggests that the extract, which contains active compounds such as flavonoids, phenolics, and tannins, may act as a stabilizing or complexing agent that inhibits crystal growth during synthesis [23]. This mechanism is commonly referred to as green synthesis, wherein biomolecules from natural sources function as capping agents to control particle size and morphology [24]. Differences in crystallinity are also reflected in the Degree of Crystallinity (DoC), calculated as the ratio of the crystalline peak area to the total area of the XRD curve. For pure ZnO, the DoC increased significantly from 60.02% at 400°C to 80.6% at 800°C. In contrast, ZnO synthesized with extract showed a more modest increase, from 49.9% to only 52.4%, indicating that the presence of plant extract hinders atomic ordering in the

crystal lattice and results in lower crystallinity. Overall, the XRD results indicate that higher calcination temperatures enhance the crystallinity and crystallite size of ZnO while reducing structural defects. Conversely, the addition of *Melaleuca leucadendra*(L) leaf extract leads to smaller crystallites and lower crystallinity.

3.4 Particle Size Distribution Analysis (PSA/DLS) Analysis

Figure 4 shows the particle size distribution measurements of ZnO samples using PSA/DLS, highlighting the significant influence of *Melaleuca leucadendra*(L) leaf extract on particle size.

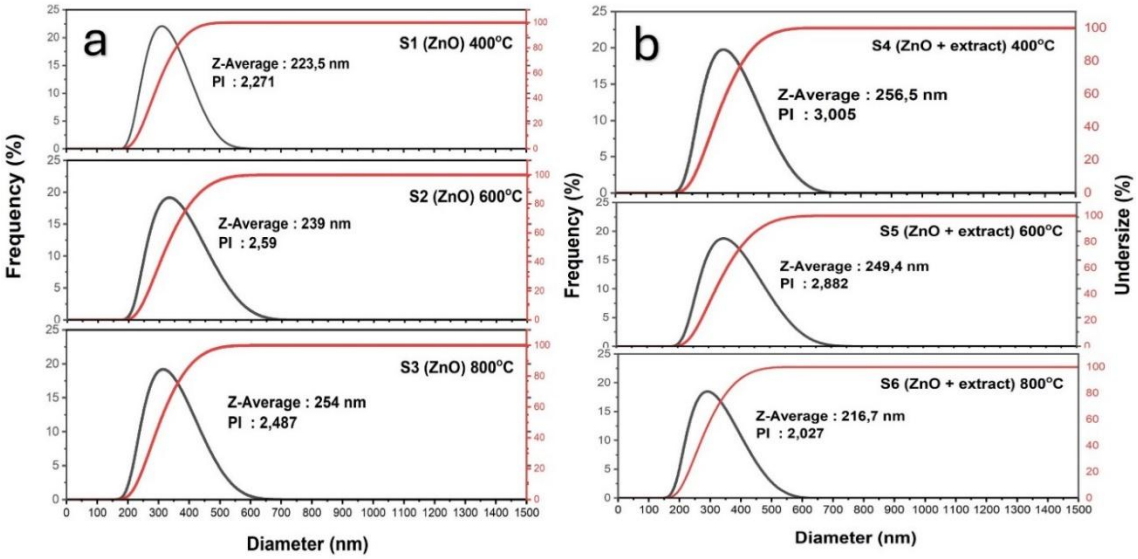

Figure 4. Particle size analysis on ZnO samples without extract (Figure 4a) and with *Melaleuca leucadendra*(L) leaf extract (Figure 4b) at 400°C, 600°C, and 800°C calcination temperature variations.

As illustrated in Figure 4a, the ZnO samples synthesized without extract (S1–S3) exhibit an increasing trend in average particle size (Z-Average) from 223.5 nm to 254 nm with increasing calcination temperature from 400°C to 800°C. The corresponding Polydispersity Index (PI) values range from 2.27 to 2.59. The consistently high PI values (>0.7) suggest a polydisperse distribution and potential particle agglomeration. This observation aligns with the findings of Wang (2004), which reported that elevated temperatures promote grain diffusion and particle aggregation [25]. In contrast, Figure 4b shows that the ZnO samples synthesized with plant extract (S4–S6) follow a different trend. At lower temperatures, the particles tend to be larger (256 nm), but at the highest temperature (800°C), the average particle size decreases to 216.7 nm, accompanied by the lowest PI value (2.03). This indicates a narrower size distribution and suggests a more controlled level of agglomeration.

These results are consistent with the green synthesis mechanism described by Ibrahim (2015) and other studies on green-synthesized ZnO, where biomolecules such as flavonoids and polyphenols act as capping agents, effectively limiting excessive particle growth and agglomeration [26]. Although the particle sizes in this study are relatively large (over 200 nm), the observed decrease in size and PI at 800°C supports the idea that the presence of extract enhances particle homogeneity and stability. Furthermore, according to Vasquez et al. (2016), particles with diameters below 1000 nm are still considered acceptable as nanocarriers in pharmaceutical applications [27].

3.5 Zeta Potential Analysis

Figure 5(a–b) displays the zeta potential measurements of ZnO samples synthesized without and with *Melaleuca leucadendra*(L) leaf extract. All samples exhibit negative zeta potential values ranging from −43 to −57 mV, indicating good electrostatic stability in suspension. According to the literature, zeta potential values with absolute magnitudes greater than 30 mV (either positive or negative) are generally considered to reflect high stability due to strong electrostatic repulsion that prevents particle agglomeration [28].

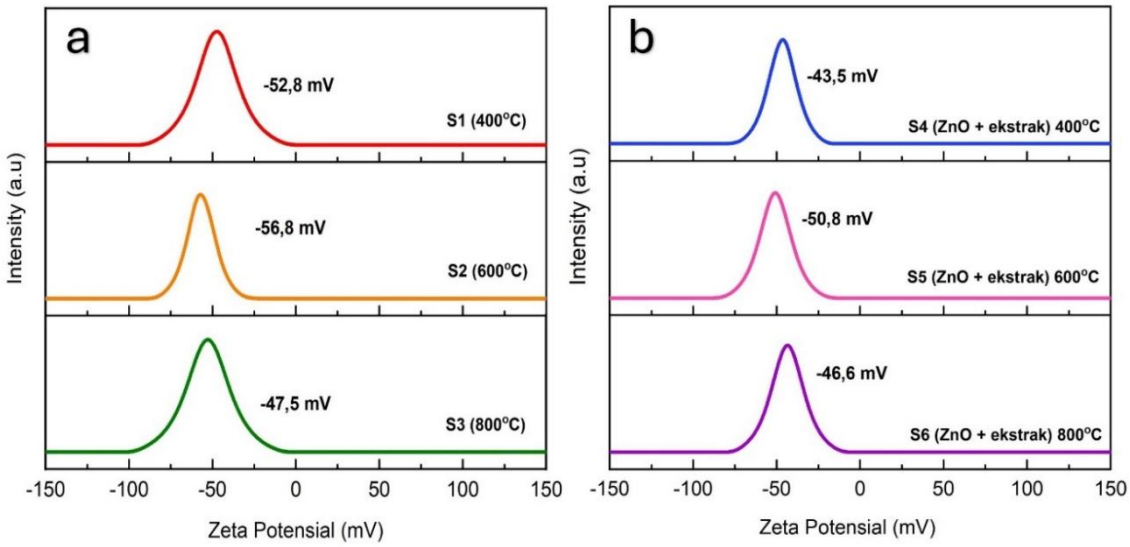

Figure 5. Zeta potential of ZnO samples without extract (Figure 5a) and with *Melaleuca leucadendra*(L) leaf extract (Figure 5b) at 400°C, 600°C, and 800°C calcination temperature variations.

As shown in Figure 5a, the pure ZnO samples (S1–S3) reach the most negative value of −56.8 mV at 600°C, suggesting optimal electrostatic stabilization at this calcination temperature. However, the value decreases to −47.5 mV at 800°C, possibly due to increased dislocation density and larger crystallite size, which reduce the surface charge density. This trend is in line with theoretical principles suggesting that crystal growth may reduce surface stability due to a decrease in active surface area. In contrast, Figure 5b shows that the ZnO samples synthesized with plant extract (S4–S6) exhibit slightly less negative zeta potential values (−43.5 mV to −50.8 mV), but still above the −30 mV threshold for colloidal stability. The slightly lower absolute values may be attributed to the adsorption of biomolecules as flavonoids and phenols, which create a molecular shell around the particle surface. This adsorption may partially mask the surface charge while still maintaining sufficient repulsive forces to ensure dispersion stability. These findings are consistent with previous studies on biosynthesized ZnO using Punica granatum and Cymbopogon citratus extracts, where zeta potentials remained strongly negative (−42 to −62 mV) due to surface-bound biomolecules. So, both types of ZnO samples demonstrate high colloidal stability, with the pure ZnO at 600°C showing the highest zeta potential magnitude.

3.6 Photoluminescence and Optical Band Gap Analysis

Figure 6 shows the photoluminescence (PL) spectra of ZnO samples excited at a wavelength of 254 nm. The UV-Vis spectra revealed maximum absorption peaks between 352.5–356 nm for all ZnO samples, both with and without the addition of

Melaleuca leucadendra(L) leaf extract. These absorption peaks fall within the near-ultraviolet (near-UV) region, which is a typical characteristic of ZnO, a wide band gap n-type semiconductor. Based on the shift in peak positions, the energy band gap (Eg) values were estimated using the formula Eg = 1240/λ, resulting in calculated values ranging from 3.40 eV to 3.52 eV. The highest band gap was observed in the pure ZnO sample calcined at 800 °C (S3), at 3.52 eV, while the lowest was found in the extract-assisted ZnO sample at 600 °C (S5), at 3.40 eV.

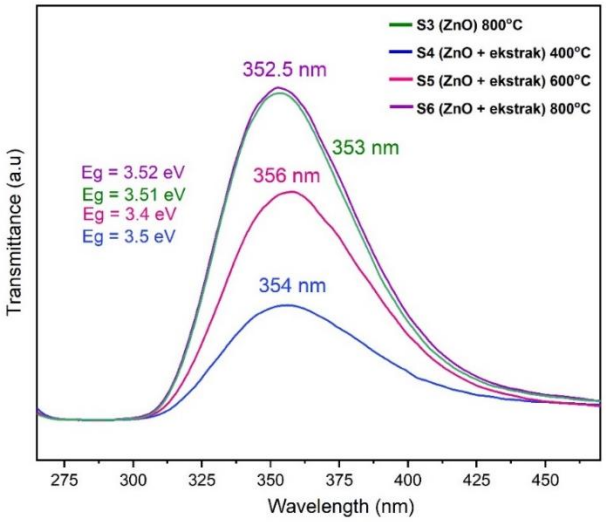

Figure 6. Photoluminescence spectra of samples with the addition of *Melaleuca leucadendra*(L) leaf extract at calcination temperatures of 400°C. 600°C. and 800°C and without *Melaleuca leucadendra*(L) leaf extract at calcination temperature of 800°C.

The decrease in band gap energy observed in sample S5 indicates a red-shift phenomenon, possibly caused by the presence of structural defects or the formation of sub-bandgap states due to incomplete crystallization or residual organic adsorbates from the plant extract. In contrast, the highest Eg value for S3 (pure ZnO at 800°C) reflects improved crystallinity and reduced defect density, consistent with XRD and PL data showing larger crystallite size, lower FWHM, and stronger PL intensity attributes associated with sharper and cleaner band edges [29]. This spectral shift and variation in band gap values are commonly reported in ZnO synthesized via green synthesis methods. Bushra et al. reported that the presence of plant-derived organic molecules can alter the surface chemistry of ZnO particles, potentially reducing band gap energy due to weakened quantum confinement or the formation of intermediate energy states between the valence and conduction bands [30]. Moreover, phenolic and flavonoid compounds acting as capping agents may stabilize small particles but also interact with the ZnO surface, inducing band gap modifications.

4. Conclusions

ZnO nanoparticles were successfully synthesized via a sol-gel method with and without the addition of *Melaleuca leucadendra*(L) leaf extract at calcination temperatures of 400°C, 600°C, and 800°C. Characterization results revealed that calcination temperature plays a crucial role in determining the crystallite size and stability of ZnO. XRD characterization showed that all samples had a hexagonal wurtzite crystal structure, with increasing temperature resulting in higher crystallinity and larger crystallite sizes, reaching 78.71 nm at 800°C for the sample without extract and 32.81 nm for the sample

with extract. PSA results showed that 800°C led to more uniform particle size distribution, particularly in extract-assisted samples. All samples exhibited high zeta potential values, indicating good colloidal stability, with the highest stability observed at 600°C. UV-Vis spectra demonstrated a band gap increase with temperature, reaching 3.52 eV for pure ZnO at 800°C, suggesting enhanced crystal order and fewer defects. Overall, 800°C was found to be the optimal temperature for producing high-quality ZnO crystals. The use of *Melaleuca leucadendra*(L) leaf extract served as a green capping agent, aiding in defect suppression. This green synthesis approach shows promising potential for applications in photocatalysis, sensing, and other functional material fields.

Acknowledgments

This work was supported by the BIMA-PER DIKTI research program with grant number 3018/UN6.3.1/PT.00/2023 from the Ministry of Education, Culture, Research and Technology. Additionally, this work was also supported by the Academic Leadership Grant (ALG) research program with grant numbers 1549/UN6.3.1/PT.00/2023 and 1459/UN6.3.1/PT.00/2024 from the Directorate of Research and Community Service, Padjadjaran University, Indonesia.

References

1. S. Raha, M. Ahmaruzzaman, ZnO nanostructured materials and their potential applications: progress, challenges and perspectives, Nanoscale Adv, 4 (2022) 1868–1925. https://doi.org/10.1039/D1NA00880C
2. G.K. Dalapati, H. Sharma, A. Guchhait, N. Chakrabarty, P. Bamola, Q. Liu, et al., Tin oxide for optoelectronic, photovoltaic and energy storage devices: A review, J. Mater. Chem. A, 9 (2021) 16621–16684. https://doi.org/10.1039/D1TA01291F
3. A. Benami, T. Ouslimane, L. Et taya, A. Sohani, Comparison of the effects of ZnO and TiO_2 on perovskite solar cell performance via SCAPS 1D, J. Nano Electron. Phys., 14 (2022) 1–5. https://doi.org/10.21272/jnep.14(1).01033
4. B. Szczęśniak, J. Choma, M. Jaroniec, Recent advances in mechanochemical synthesis of mesoporous metal oxides, Mater. Adv., 2 (2021) 4325–4339. https://doi.org/10.1039/D1MA00073J
5. G. Matyszczak, K. Krawczyk, A. Yedzikhanau, K. Głuc, M. Szymajda, A. Sobiech, Z. Gackowska, Sonochemical synthesis of low dimensional nanostructures and their applications - a review, Materials (Basel), 17 (2024) 5488. https://doi.org/10.3390/ma17225488
6. S.D. Dhas, P.S. Maldar, M.D. Patil, K.M. Hubali, U.V. Shembade, S.B. Abitkar, M.R. Waikar, R.G. Sonkawade, G.L. Agawane, A.V. Moholkar, Hydrothermal synthesis of mesoporous $NiMnO_3$ nanostructures for supercapacitor application: effect of electrolyte, J. Energy Storage, 43 (2021) 102277. https://doi.org/10.1016/j.est.2021.102277
7. R. Yarbrough, K. Davis, S. Dawood, H. Rathnayake, A sol gel synthesis to prepare size and shape controlled mesoporous nanostructures of binary (II–VI) metal oxides, RSC Adv., 10 (2020) 12345–12356. https://doi.org/10.1039/D0RA01778G
8. D. Navas, S. Fuentes, A. Castro Alvarez, E. Chavez Angel, Review on sol gel synthesis of perovskite and oxide nanomaterials, Gels, 7 (2021) 275. https://doi.org/10.3390/gels7040275
9. R. Sharma, A.D. Acharya, S.B. Shrivastava, T. Shripathi, V. Ganesan, Preparation and characterization of transparent NiO thin films deposited by spray pyrolysis technique, Optik (Stuttg.), 125 (2014) 5127–5132. https://doi.org/10.1016/j.ijleo.2014.07.104

10. S. Wulan, F. Abrar, I.W. Fathonah, Green synthesis of ZnO nanoparticles as photocatalyst for methylene blue degradation, e Proceeding Eng., 6 (2019) 5092–5099.
11. A. Trisnaningtyas, A. Muhtadun, Review: green synthesis of ZnO nanoparticles, (2022)
12. P.K. Pino, E.L. Regalado, J.L. Rodríguez, M.D. Fernández, Phytochemical analysis and in vitro free radical scavenging activities of essential oils from leaf and fruit of *Melaleuca leucadendra* L., Chem. Biodivers., 7 (2010) 2281–2288. https://doi.org/10.1002/cbdv.201000181
13. P. Sharma, M. Urfan, R. Anand, M. Sangral, H.R. Hakla, S. Sharma, R. Das, S. Pal, M. Bhagat, Green synthesis of zinc oxide nanoparticles using Eucalyptus lanceolata leaf litter: characterization, antimicrobial and agricultural efficacy in maize, Physiol. Mol. Biol. Plants, 28 (2022) –. https://doi.org/10.1007/s12298-022-01136-0
14. M. Hafeez, A. Ghazal, J. Khan, P. Ahmad, M.U. Khandaker, H. Osman, S. Alamri, Eucalyptus globulus extract assisted fabrication of copper oxide/zinc oxide nanocomposite for photocatalytic applications, Crystals, 12 (2022) 1153. https://doi.org/10.3390/cryst12081153
15. M.U. Sadiq, A. Shah, A. Haleem, S.M. Shah, I. Shah, Eucalyptus globulus mediated green synthesis of environmentally benign metal based nanostructures: a review, Nanomaterials, 13 (2023) 2019. https://doi.org/10.3390/nano13132019
16. S. Muthusamy, S. Bharatan, S. Sivaprakasam, R. Mohanam, Effect of deposition temperature on Zn interstitials and oxygen vacancies in RF sputtered ZnO thin films and TFTs, Materials (Basel), 17 (2024) 15153. https://doi.org/10.3390/ma17215153
17. F.G. Fetisov, X ray diffraction methods for structural diagnostics of materials: progress and achievements, Phys. Uspekhi, 63 (2020) 1052–1075. https://doi.org/10.3367/UFNe.2018.10.038435
18. Z. Villagrán, L.M. Anaya Esparza, C.A. Velázquez Carriles, J.M. Silva Jara, J.M. Ruvalcaba Gómez, E.F. Aurora Vigo, E. Rodríguez Lafitte, N. Rodríguez Barajas, I. Balderas León, F. Martínez Esquivias, Plant based extracts as reducing, capping, and stabilizing agents for the green synthesis of inorganic nanoparticles, Resources, 13 (2024) 60070. https://doi.org/10.3390/resources13060070
19. S.A. Neamah, S. Albukhaty, I.Q. Falih, Y.H. Dewir, H.B. Mahood, Biosynthesis of zinc oxide nanoparticles using Capparis spinosa L. fruit extract: characterization, biocompatibility, and antioxidant activity, Appl. Sci., 13 (2023) 116604. https://doi.org/10.3390/app13116604
20. X.T. Tran, T.T.L. Bien, T.V. Tran, T.T.T. Nguyen, Biosynthesis of ZnO nanoparticles using aqueous extracts of Eclipta prostrata and Piper longum: characterization and assessment of antioxidant, antibacterial, and photocatalytic properties, Nanoscale Adv., 6 (2024) 4885–4899. https://doi.org/10.1039/D4NA00488F
21. A.A. Chaudhari, U.J. Tupe, A.V. Patil, C.G. Dighavkar, Synthesis and characterization of zinc oxide nanoparticles using green synthesis method, 10 (2022) 302.
22. W.Z. Wang, S. Mei, P. Manivel, H. Ma, X. Chen, Zinc oxide nanoparticles synthesized using coffee leaf extract assisted with ultrasound as nanocarriers for mangiferin, Curr. Res. Food Sci., 5 (2022) 100501. https://doi.org/10.1016/j.crfs.2022.05.002
23. K.B.H. Kiani, Q. Ajmal, N. Akhtar, I.U. Haq, M.A. Abdel Maksoud, A. Malik, M. Aufy, N. Ullah, Biogenic synthesis of zinc oxide nanoparticles using Citrullus

colocynthis for potential biomedical applications, Plants, 12 (2023) 203. https://doi.org/10.3390/plants12020362
24. I.H.M. Wulan, Green synthesis nanoparticle ZnO sebagai fotokatalis untuk mendegradasi metilen biru, e Proceeding Eng., 6 (2019) 5092–5099.
25. T.Z. Khoshraftar, A.A. Safekordi, A. Shamel, M. Zaefizadeh, Synthesis of natural nanopesticides with the origin of Eucalyptus globulus extract for pest control, Green Chem. Lett. Rev., 12 (2019) 286–298.
26. F.G. Easmin, I.S.M. Zaidul, K. Ghafoor, S. Ferdosh, J. Jaffri, M.E. Ali, V. Perumal, F.Y. Al Juhaimi, V. Mirhosseini, A. Khatib, Rapid investigation of α glucosidase inhibitory activity of Phaleria macrocarpa extracts using FTIR ATR based fingerprinting, J. Food Drug Anal., 25 (2017) 306–315.
27. F. Hafeez, A. Ghazal, J. Khan, P. Ahmad, M.U. Khandaker, H. Osman, S. Alamri, Eucalyptus globulus extract assisted fabrication of copper oxide/zinc oxide nanocomposite for photocatalytic applications, Crystals, 12 (2022) 1153. https://doi.org/10.3390/cryst12081153
28. S. Ali, A. Haleem, S.M. Shah, I. Shah, Eucalyptus globulus mediated green synthesis of environmentally benign metal based nanostructures: a review, Nanomaterials, 13 (2023) 2019. https://doi.org/10.3390/nano13132019
29. A.A. Chaudhari, U.J. Tupe, A.V. Patil, C.G. Dighavkar, Synthesis and characterization of zinc oxide nanoparticles using green synthesis method, 10 (2022) 302.
30. W.Z. Wang, S. Mei, P. Manivel, H. Ma, X. Chen, Zinc oxide nanoparticles synthesized using coffee leaf extract assisted with ultrasound as nanocarriers for mangiferin, Curr. Res. Food Sci., 5 (2022) 100501. https://doi.org/10.1016/j.crfs.2022.05.002